

The Physics of Clumpy AGN Tori

Thomas Beckert⁽¹⁾, Sebastian F. Hönig⁽¹⁾, Makoto Kishimoto⁽¹⁾,
M. Almudena Prieto⁽²⁾, Gerd Weigelt⁽¹⁾

(1) MPI für Radioastronomie, Bonn, Germany; (2) IAC, Tenerife, Spain



MAX-PLANCK-GESELLSCHAFT

Dusty tori in the unified model of AGN

The unified model of active galactic nuclei (AGN) explains the differences between type 1 and type 2 AGN with aspect-angle-dependent obscuration by a geometrically thick dusty torus:

- The model emerged from the interpretation of weak polarized broad emission lines hidden by strong narrow lines observed in the Seyfert 2 nucleus of NGC 1068 (Miller & Antonucci 1983, ApJ, 271, L7).
- In the simplest unification scheme all Seyfert 2 nuclei harbor an obscured Seyfert 1 core.
- **The ratio of type 1s to 2s measures the thickness of the obscuring torus $\Rightarrow H/R \sim 1$.**
- The inner boundary of the torus is set by dust destruction at $R \sim 0.5 \text{ pc } L_{45}$ which depends on the AGN luminosity $L = 10^{45} L_{45} \text{ erg/s}$ and dust chemistry.
- Krolik & Begelman (1988, ApJ 329, 702) showed that tori are composed of a large number of clouds.
- Clumpiness has a strong influence on the appearance of tori in infrared observations as shown by radiative transfer calculations (Nenkova et al. 2002, ApJ 570, L9).

Cloud distribution and cloud properties in the torus

We have implemented an equilibrium model for cold, molecular and dusty clouds in the environment of an active nucleus (Vollmer et al. 2004, A&A, 413, 949). The clouds in the torus are assumed quasi-stable and experience frequent cloud-cloud collisions. The mass and size of the largest clouds in the torus is limited by tidal forces in the gravitational potential of the galactic nucleus. We assume a balance of internal pressure against the clouds self-gravity (Jeans-limit). The important parameter for torus dynamics and the appearance in radiative transfer calculations is the *vertical optical depth* for intercepting a cloud

$$\tau = \int l_{\text{coll}}^{-1} dz, \quad (1)$$

where l_{coll} is the mean free path of clouds in the torus. We derived the distribution of clouds and cloud velocities (Beckert & Duschl 2004, A&A 426, 445).

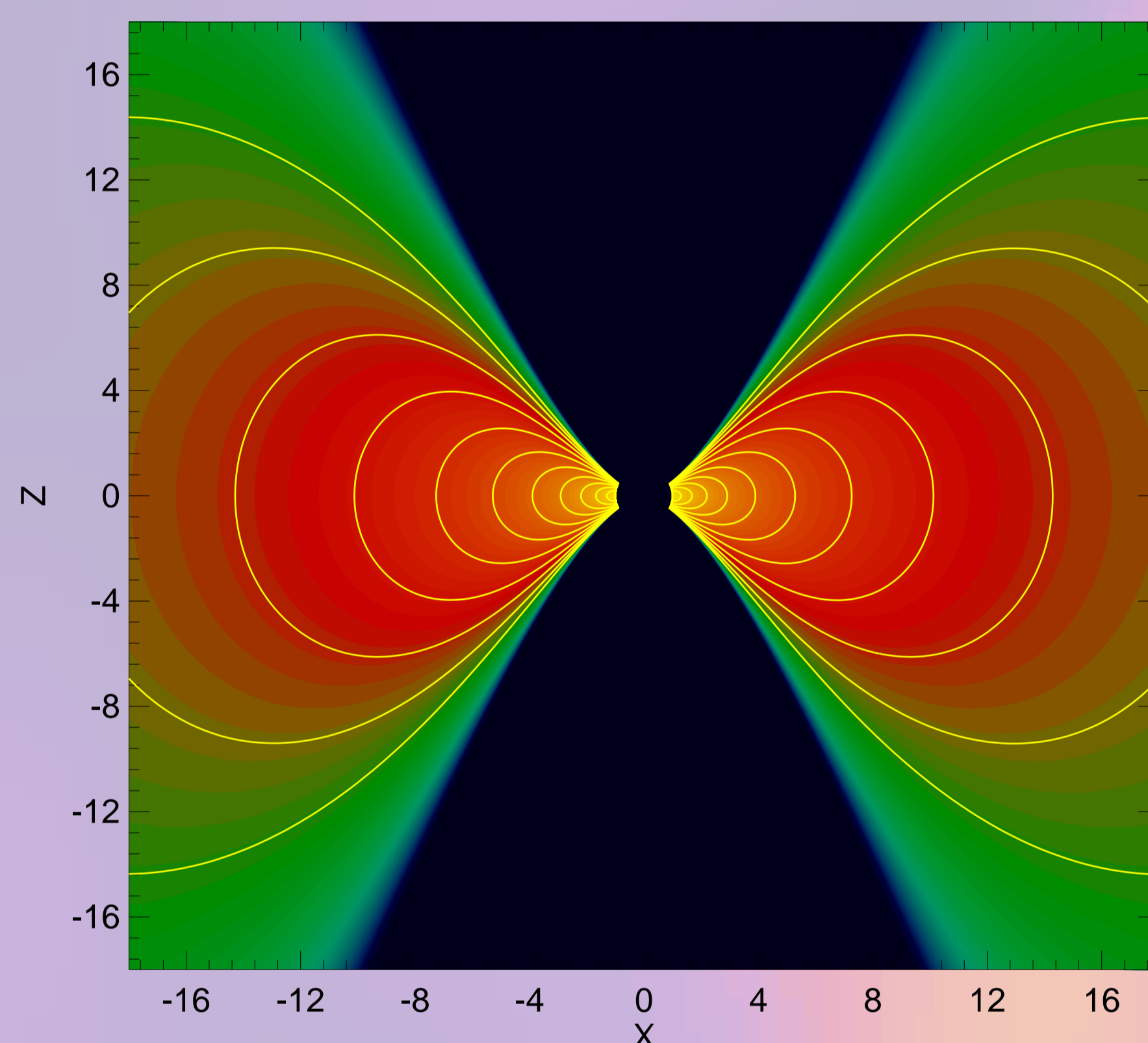


Figure 1: Model for the Seyfert nucleus of NGC 1068: Meridional cut through the probability density distribution of finding a cloud in the torus (red: high probability). The distribution leaves room for an outflow along the polar axis. The spatial scale is in units of the torus inner radius. The mean number of clouds along a line of sight to the center drops below unity for angles larger than 40° from the midplane ($Z = 0$). The radial structure is derived from a stationary accretion scenario.

In order to obscure the central engine for lines of sight passing through the torus the depth parameter τ defined in Eq. (1) has to be $\tau \sim 1$. Because τ is also a dimensionless collision frequency $\tau \sim \omega_c/\Omega$, this implies that cloud-cloud collisions are frequent. Cloud collisions allow angular momentum redistribution between the clouds. Like in a standard accretion disk picture, transport of angular momentum will lead to mass transport towards the central black hole and feeding of the central engine.

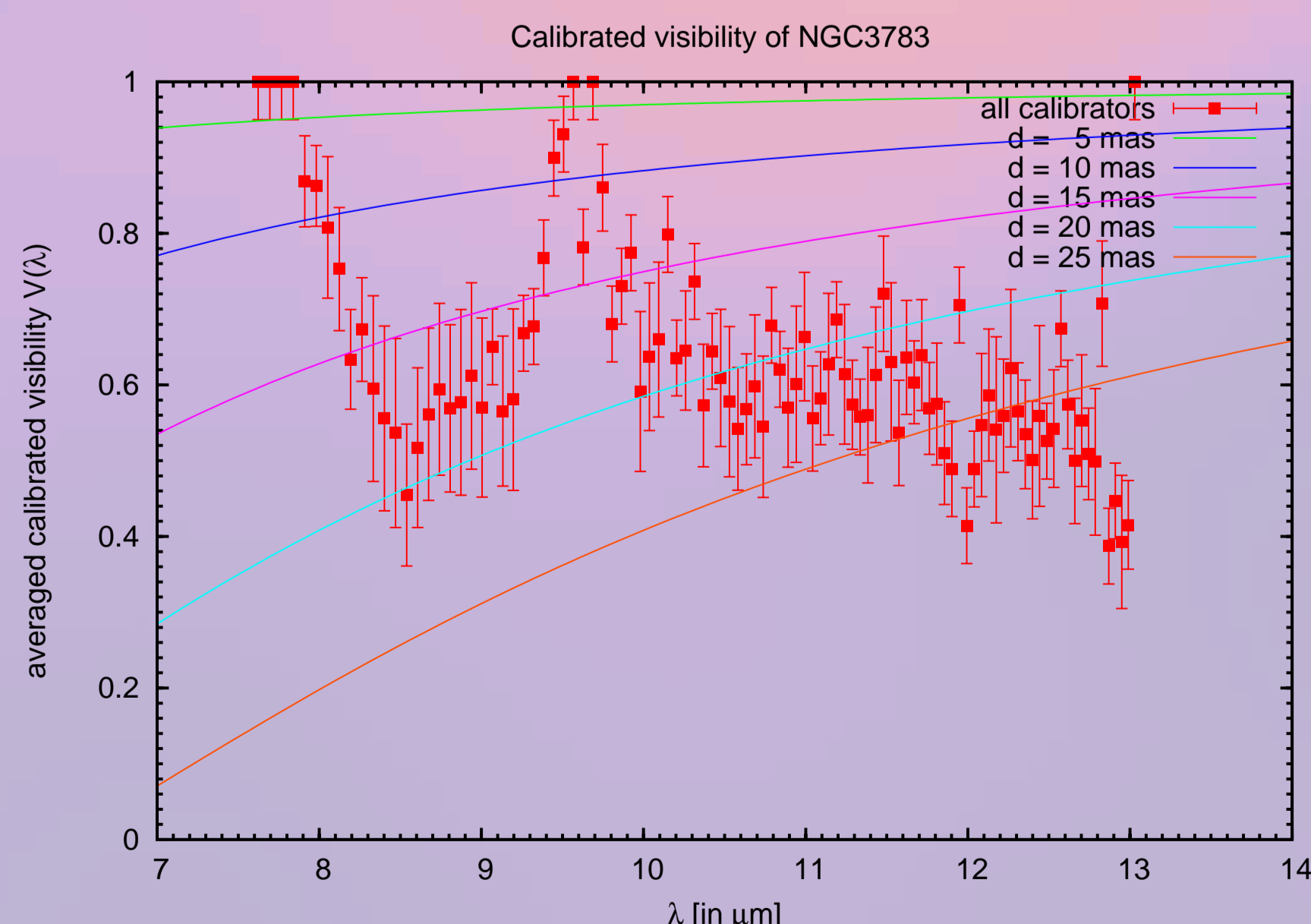
Prime examples and interferometric results

NGC 1068 has been successfully resolved using ESO's VLT Interferometer (VLTI) in the K -band (VINCI instrument at $2.2 \mu\text{m}$; Wittkowski et al. 2004, A&A 418, L39) and with VLTI/MIDI in the N -band ($8 - 13 \mu\text{m}$; Jaffe et al. 2004, Nature 429, 47). **The torus emission has already been resolved by single telescope speckle interferometry (Wittkowski et al. 1998, A&A 329, L45; Weigelt et al. 2004, A&A, 425, 77) resulting in a core size of $18 \times 39 \text{ mas}$.** This is comparable to the N -band interferometric sizes. See discussion on the right.

Circinus: The nucleus of this bright Seyfert 2 has been resolved by K -band adaptive optics observations (Prieto et al. 2004, ApJ, 614, 135). The available VLTI/MIDI data indicate a highly resolved N -band structure (Tristram et al. 2006, IAU 238, 54). The nucleus shows a $\sim 10 \mu\text{m}$ silicate feature in absorption.

NGC 3783: Spectro-interferometry using ESO's VLTI/MIDI in the N -band shows no $10 \mu\text{m}$ -feature from silicate dust.

Figure 2: Visibilities from May 2005 for a baseline of 65 m indicate a *partly resolved central source*. The lines indicate uniform disk diameters between 5–25 mas. Please note the strong atmospheric ozone band around $9.5 \mu\text{m}$ (Beckert et al.; in preparation).



NGC 4151: For this bright type 1 nucleus Swain et al. (2003, ApJ, 596, L163) derived a high visibility ($V^2 = 0.84 \pm 0.06$ at 83 m baseline) with the Keck interferometer in K -band. The correlated flux may come from the accretion disk proper or indicates a very small dust destruction radius (see implications on the right).

Centaurus A: Recent VLTI/MIDI observations in the $8-13 \mu\text{m}$ window (Meisenheimer et al., submitted) indicate a compact, possibly unresolved nucleus in the MIR. The nuclear SED (including upper limits to the size) can be modeled by a compact dusty torus or a non-thermal synchrotron source at base of the prominent radio/X-ray jet with strong foreground absorption ($A_V \sim 18$).

Results of radiative transfer calculations

The radiative transfer problem is split in two steps (Hönig et al. 2006, A&A, 452, 459): First, we simulate individual clouds and create a database of cloud models. Secondly, we pick a realization of the cloud distribution shown in Fig. 1 to distribute these clouds and build up the torus.

• Monte Carlo simulation of individual dust clouds:

We use a Monte Carlo radiative transfer code to simulate individual dusty clouds at various distances from the AGN. From our modeling, we obtain properties of the radiation field emitted by each cloud. We must distinguish between (1) clouds which directly see the AGN, and (2) clouds which are not directly exposed to the central AGN, (which see the diffuse radiation field of the surrounding clouds).

• Radiative transport of the cloud emission through the torus:

The *accretion scenario of clumpy tori* presented above provides the *cloud size* and *optical depth* for each position within the torus. We combine the MC-results for individual clouds with the shadowing effects by other clouds to obtain simulated torus SEDs, spectra and images.

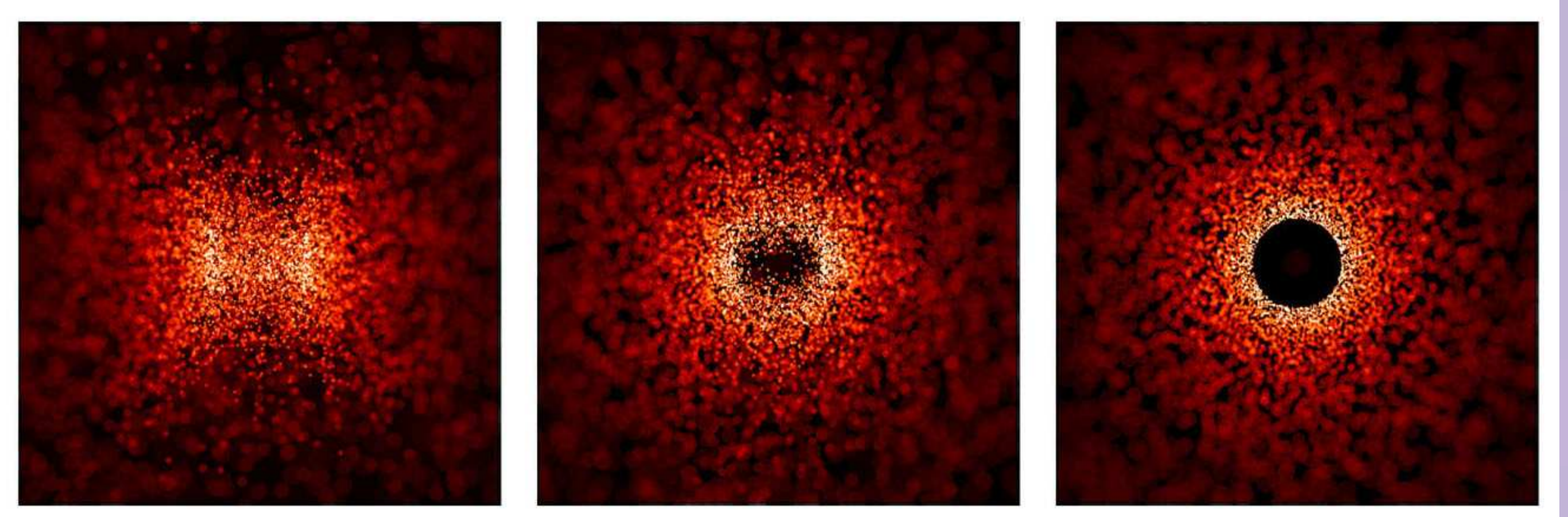


Figure 3: MIR N -band model images of the brightness distribution from our 3-D radiative transfer calculations for clumpy AGN tori (Hönig et al. 2006). From left to right, the images represent torus inclinations of $i = 90^\circ$ (edge-on), $i = 30^\circ$, and $i = 0^\circ$ (face-on).

The torus model allows us to constrain basic physical properties of the torus: *AGN bolometric luminosity, inclination, radial and vertical dust distribution, and dust chemistry*. Fig. 4 shows that the trend of deeper silicate feature with growing baseline for NGC 1068 is reproduced.

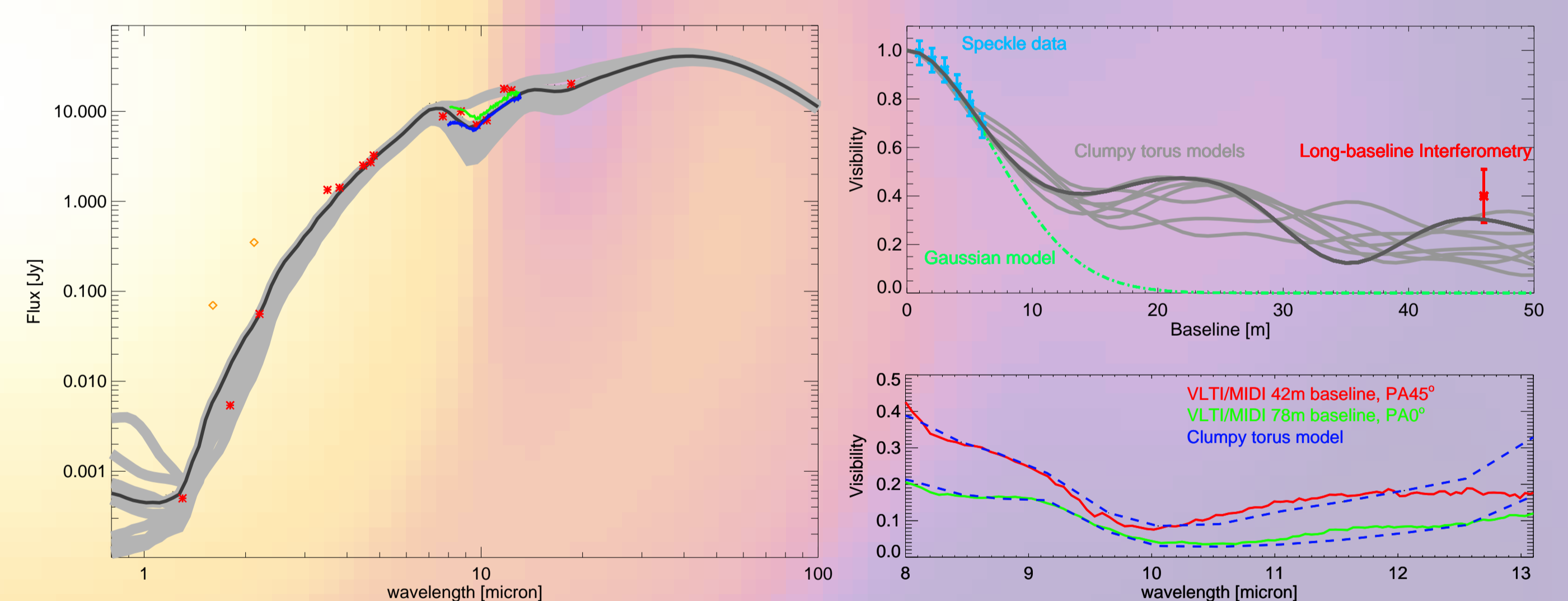


Figure 4: Comparison between observed high-resolution data of NGC 1068 and the clumpy torus model. **Left: SED:** Red: high-resolution photometry; Diamonds: speckle observations; Green curve: total MIR flux from VLTI/MIDI; Blue curve: Gemini MIR spectrum (Mason et al. 2006, ApJ, 640, 612). The shaded area shows the range of variations of model SEDs obtained for 10 different cloud arrangements. The dark grey curve shows the best-fitting model. **Top right:** K -band visibilities from interferometry of NGC 1068 (speckle: Weigelt et al. 2004; Long-baseline: Wittkowski et al. 2004), together with the clumpy torus model. **Bottom right:** VLTI/MIDI spectro-interferometry of NGC 1068 (Jaffe et al. 2004). Red: Visibility at $B = 42 \text{ m}$ (PA 45°); Green: Visibility at $B = 78 \text{ m}$ (PA 0°). Blue: Model visibilities for one particular random cloud arrangement (dark grey model).

Implications

Comparison of direct imaging with K -band reverberation sizes: Theoretical prediction (Barvainis 1987, ApJ, 320, 537) of dust destruction radius gives robust estimation of inner torus boundary.

- However, the time-lag radii from near-IR reverberation measurements (Suganuma et al. 2006, 639, 46) are significantly smaller.
- **This indicates that the dust properties might be systematically different from those often assumed: Sublimation temperature $T_{\text{sub}} > 1500 \text{ K}$ and/or typical grain radius $a \gg 0.05 \mu\text{m}$.**
- Alternatives: Central engine radiation is highly anisotropic or significantly extinguished along equatorial directions before reaching the torus (M. Kishimoto et al., submitted).

AGN Tori at low and high luminosities: For low luminosities below $\sim 10^{42} \text{ erg/s}$, the torus changes its characteristics and obscuration becomes insufficient.

At high luminosities (bright Seyfert nuclei & QSOs) the largest clouds in the torus become gravitationally unbound if the AGN radiates close to the classical Eddington limit.

\Rightarrow **The effective scale height of the torus decreases with luminosity, $H/R \propto L^{-1/4}$.**

The resulting L -dependence of type 1 vs 2 ratio is consistent with an analysis of several AGN surveys by Simpson (2005, MNRAS, 360, 565).

The clumpy torus can account for broad-line AGN with high X-ray column densities, and more such objects should be found at high rather than at low luminosities. (Hönig & Beckert, submitted).